XLIII CILAMCE
21–25, November, 2022
FOZ DO IGUAÇU – PR – BRAZIL

Influence of Soil-Structure Interaction (SSI) on the performance of the Connected Control Method (CCM)

Luis A. P. Peña[1], Suzana M. Avila[2], Graciela N. Doz[3]

[1]*Department of Technology, School of Architecture and Urbanism, University of Brasilia*
Campus Universitário Darcy Ribeiro - ICC Norte, 70904-970, Brasília/DF, Brazil
alejandrop@unb.br
[2]*Engineering Faculty Gama, Gama Engineering College, University of Brasilia*
St. Leste Projeção A - Gama Leste, 72444-240, Brasília/DF, Brazil
avilas@unb.br
[3]*Department of Civil Engineering, Faculty of Technology, University of Brasilia*
Campus Universitário Darcy Ribeiro - Asa Norte, 70910-900, Brasília/DF, Brazil
graciela@unb.br

Abstract. The Connected Control Method (CCM) has proved to be an effective strategy to mitigate the building vibrational response and prevent inter-building pounding effects. In this technique, adjacent buildings are linked together by means of coupling devices to provide appropriate reaction control forces. The application of the CCM using different kinds of passive, active, and semiactive linking devices has been investigated with positive results. It should be noted that most of such research considered the adjacent buildings supported on a fixed base. Nonetheless, every structure generally interacts with the surrounding soil. This process is known as soil-structure interaction (SSI) and there are still few studies in literature about its influence on the CCM and the mathematical formulation regarding the problem is merely incipient. Thus, this work aims to evaluate SSI influence on the performance of this control technique, besides presenting a simple analysis methodology to this type of problem. For this purpose, two buildings connected models supported on a fixed and flexible base are compared. The buildings are modeled as shear buildings and the soil is simulated by a discrete model representing a viscoelastic homogeneous half-space. The results are compared in a way to evaluate SSI influence on coupled buildings dynamic behavior. The numerical analysis was performed in GNU Octave software.

Keywords: dynamic, vibration control, optimization, soil-structure interaction, connected control method

1 Introduction

The impact between two neighboring high buildings, during severe earthquakes in the past, caused significant damages and loss of lives. In order to avoid these problems, in the beginning of seventies various researchers proposed to connect neighboring structures using cable connecting devices. This technique called structural coupling or Connected Control Method (CCM) [1] has proved to be effective on minimizing impact possibilities between two neighboring structures, besides of mitigating its dynamical responses.

Many experimental and numerical studies have shown that coupling adjacent buildings using passive devices reduces the possibilities of pounding between them [2–5] and improves their seismic performances [6–11]. Most of such research used fluid viscous, viscous elastic, hysteretic or friction-based dampers as the connecting device and considered the buildings supported on a fixed base. One of the main conclusions was that the connecting devices are effective if the two adjacent structures have different dynamic properties. In addition, these elements can increase the energy dissipation capacity of the structural system according to its mechanical properties and its position between the adjacent buildings.

In general, every structure interacts with the surrounding soil. This process is known as soil-structure interaction (SSI) [12]. During earthquakes, structures interact with soil in its surroundings, imposing strains to it. These deformations, however, cause movements in the supports or in the interface zone between the ground and the structure, which are different from the movement of the free ground surface. These interactions substantially modify the dynamic responses of the buildings.

Nonetheless, the seismic assessment of multi-storey buildings is usually based on the assumption that they are mounted on a rigid structure medium and that the effects of soil-structure interaction (SSI) are disregarded. However, the consequences and severities of neglecting the effects of SSI have been demonstrated by several researchers [13–16]. Moreover, there are still few studies in the literature about SSI influence on the CCM and the mathematical formulation regarding the problem is merely incipient [17].

Thus, this work aims to evaluate SSI influence on the performance of this control technique, besides presenting a simple analysis methodology to this type of problem. It should be mentioned that only the inertial part of SSI is considered. For this purpose, two buildings connected models supported on a fixed and flexible base are compared. The buildings are modeled as shear buildings and the soil is simulated by a discrete model representing a viscoelastic homogeneous half-space. This discrete model has already been implemented in the literature, presenting coherent results [18–22]. Likewise, it is assumed that the separation of the buildings has enough space to allow the installation of some connection devices between them.

The numerical analysis was performed in two stages through GNU Octave software. In the first stage an optimization study was performed using the Particle Swarm Optimization [23] in a way to set the connecting device properties, calculating the minimum inter-story drift of the coupled system considering a fixed base. A second stage is performed, now considering a flexible base to the coupled system, and setting the optimum properties calculated previously. Finally, all the results are compared in a way to evaluate SSI influence on coupled buildings dynamic behavior. The records of the ground acceleration corresponding to El Centro, Kobe, and Northridge earthquakes were used as seismic excitation to simulate the vibrational response of the buildings.

2 Analytical Models and Mathematical Formulation

2.1 Coupled models with fixed base

Figure 1 presents the structure model considered in this paper: a simplified shear-frame structure modeled as a lumped-mass planar system with displacements in the direction of the ground motion for the two-building coupled system.

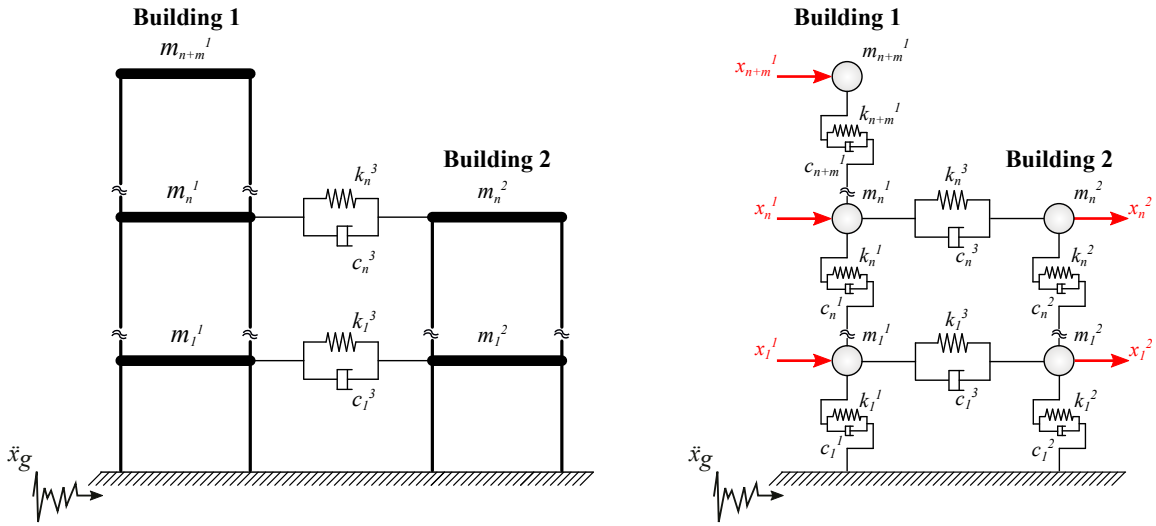

Figure 1. Coupled models with fixed base

The coupled system motion equation, when it is subjected to a seismic base acceleration $\ddot{\mathbf{x}}_g(t)$ is given by eq. (1)

$$\mathbf{M}_{bb}\ddot{\mathbf{x}}_{bb}(t) + \mathbf{C}_{bb}\dot{\mathbf{x}}_{bb}(t) + \mathbf{K}_{bb}\mathbf{x}_{bb}(t) = -\mathbf{M}_{bb}\{1\}\ddot{\mathbf{x}}_g(t) \tag{1}$$

where: the subscript *bb* in these matrices refers to adjacent buildings without SSI; $\mathbf{M}_{bb}$, $\mathbf{C}_{bb}$ and $\mathbf{K}_{bb}$ are the mass, damping and stiffness matrices of the coupled system, respectively (eq. (2)); $\mathbf{m}^1$, $\mathbf{m}^2$, $\mathbf{c}^1$, $\mathbf{c}^2$, $\mathbf{k}^1$ and $\mathbf{k}^2$ represent the diagonal mass, damping and stiffness matrices of the *Building 1* and *2*, respectively; $\hat{\mathbf{c}}$ and $\hat{\mathbf{k}}$ are the matrices that contains the damping and stiffness coefficients of the linking system c_n^3 e k_n^3 [7]; $\mathbf{x}_{bb}(t)$ is the vector of story displacements with respect to the ground (eq. (3)).

$$\mathbf{M}_{bb} = \begin{bmatrix} \mathbf{m}^1_{(n+m,n+m)} & \mathbf{0}_{(n+m,n)} \\ \mathbf{0}_{(n,n+m)} & \mathbf{m}^2_{(n,n)} \end{bmatrix} \quad \mathbf{C}_{bb} = \begin{bmatrix} \mathbf{c}^1_{(n+m,n+m)} + \hat{\mathbf{c}}_{(n+m,n+m)} & -\hat{\mathbf{c}}_{(n+m,n)} \\ -\hat{\mathbf{c}}_{(n,n+m)} & \mathbf{c}^2_{(n,n)} + \hat{\mathbf{c}}_{(n,n)} \end{bmatrix}$$

$$\mathbf{K}_{bb} = \begin{bmatrix} \mathbf{k}^1_{(n+m,n+m)} + \hat{\mathbf{c}}_{(n+m,n+m)} & -\hat{\mathbf{k}}_{(n+m,n)} \\ -\hat{\mathbf{k}}_{(n,n+m)} & \mathbf{k}^2_{(n,n)} + \hat{\mathbf{k}}_{(n,n)} \end{bmatrix} \tag{2}$$

$$\mathbf{x}_{bb} = \begin{bmatrix} x^1_1(t) & \cdots & x^1_{n+m}(t) & x^2_1(t) & \cdots & x^1_n(t) \end{bmatrix} \tag{3}$$

2.2 SSI model

In numerical analysis, the soil underlying foundation is considered as a homogeneous half-space and can be modeled by a discrete model as show in Fig. 2. Compared to more rigorous numerical methods, this model requires only a simple numerical manipulation with reasonable accuracy in engineering practice [24, 25].

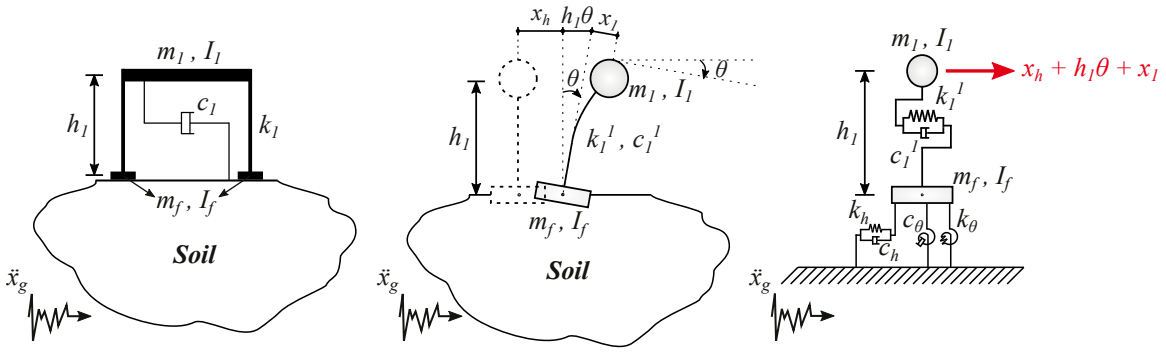

Figure 2. Soil interaction models

In this model, the horizontal (h) and the rocking (θ) degrees-of-freedom are considered as representatives of the translational and rotational motions of the foundation, respectively. Thus, x_h and θ_{h1} indicate the horizontal displacement components caused by the horizontal and the rocking motion at the roof story. The damping and stiffness soil are represented by swaying and rocking springs and dashpots with constants k_h, k_θ, c_h and c_θ, respectively. These constants are called impedance coefficients and are frequency dependent. Nonetheless, Gazetas [21] correlated these dynamic properties to static properties of soil in time domain, where the soil is represented by basic constants such as the mass density of soil (ρ), shear-wave velocity of soil (V_S) and Poisson's ratio of soil (ν) which could be easily obtained experimentally. Additionally, in this model, the foundation is treated as a circular rigid disk with radius r not considering its flexibility. The impedance coefficients are computed using the following equations

$$k_h = \frac{8\rho V_S^2 r}{2-\nu} \qquad c_h = \frac{4.6}{2-\nu}\rho V_S r^2 \qquad k_\theta = \frac{8\rho V_S^2 r^3}{3(1-\nu)} \qquad c_\theta = \frac{0.4}{1-\nu}\rho V_S r^4 \tag{4}$$

The equations of motion of the system shown in Fig. 2 considering the impedance coefficients (eq. (4)) are given by:

$$\mathbf{M}_{bs}\ddot{\mathbf{x}}_{bs}(t) + \mathbf{C}_{bs}\dot{\mathbf{x}}_{bs}(t) + \mathbf{K}_{bs}\mathbf{x}_{bs}(t) = -\mathbf{G}_{bs}\ddot{\mathbf{x}}_g(t) \tag{5}$$

$$\mathbf{M}_{bs} = \begin{bmatrix} \mathbf{m}_{s(2,2)} & \mathbf{m}_{si(2,1)} \\ \mathbf{m}_{is(1,2)} & m_1 \end{bmatrix} \quad \mathbf{C}_{bs} = \begin{bmatrix} \mathbf{c}_{s(2,2)} & \mathbf{0}_{(2,1)} \\ \mathbf{0}_{(1,2)} & c_1 \end{bmatrix} \quad \mathbf{K}_{bs} = \begin{bmatrix} \mathbf{k}_{s(2,2)} & \mathbf{0}_{(2,1)} \\ \mathbf{0}_{(1,2)} & k_1 \end{bmatrix} \tag{6}$$

$$\mathbf{m}_s = \begin{bmatrix} I_f + I_1 & h_1 m_1 \\ h_1 m_1 & m_f + m_1 \end{bmatrix} \quad \mathbf{m}_{si} = (\mathbf{m}_{is})^T = \begin{bmatrix} h_1 m_1 \\ m_1 \end{bmatrix} \quad \mathbf{c}_s = \begin{bmatrix} c_\theta & 0 \\ 0 & c_h \end{bmatrix} \quad \mathbf{k}_s = \begin{bmatrix} k_\theta & 0 \\ 0 & k_h \end{bmatrix} \tag{7}$$

$$\mathbf{G}_{bs} = \mathbf{M}_{bs} \begin{bmatrix} \mathbf{0}_{(2,1)} \\ 1 \end{bmatrix} + \begin{bmatrix} v_{s(2,1)} \\ 0 \end{bmatrix}, \; v_s = \begin{bmatrix} 0 \\ m_f \end{bmatrix} \tag{8}$$

$$\mathbf{x}_{bs} = \begin{bmatrix} x_\theta(t) & x_h(t) & x_1(t) \end{bmatrix}^T \tag{9}$$

where: the subscript *bs* in these matrices refers to building considering SSI effects; $\mathbf{M}_{bs}$, $\mathbf{C}_{bs}$ and $\mathbf{K}_{bs}$ are mass, damping and stiffness matrices of the building considering SSI effects, respectively; $\mathbf{m}_s$, $\mathbf{c}_s$ and $\mathbf{k}_s$ are the foundations soil matrices of the building; m_1, c_1 and k_1 are the mass, damping and stiffness values of the building; m_f and I_f are the mass and the mass moment of inertia of the foundation; I is mass moment of inertia of the building story; h_1 is the height from the structure base to level in the building; $\mathbf{m}_{si}$ and $\mathbf{m}_{is}$ are SSI matrices; $\mathbf{G}$ is the external force location matrix; $\mathbf{x}_{bs}(t)$ is the vector with displacements of the structures and foundations.

It should be mentioned that only the inertial part of SSI is considered in this work. The kinematic analysis of the SSI is not included assuming that the rigid foundation lies on the surface of the soil with no embedment and is subjected to vertically incident plane shear waves with particle motion in the horizontal direction.

2.3 Coupled models considering SSI

Consider now the MDF system of Fig. 1, supported by an elastic homogeneous isotropic medium, as shown in Fig. 3.

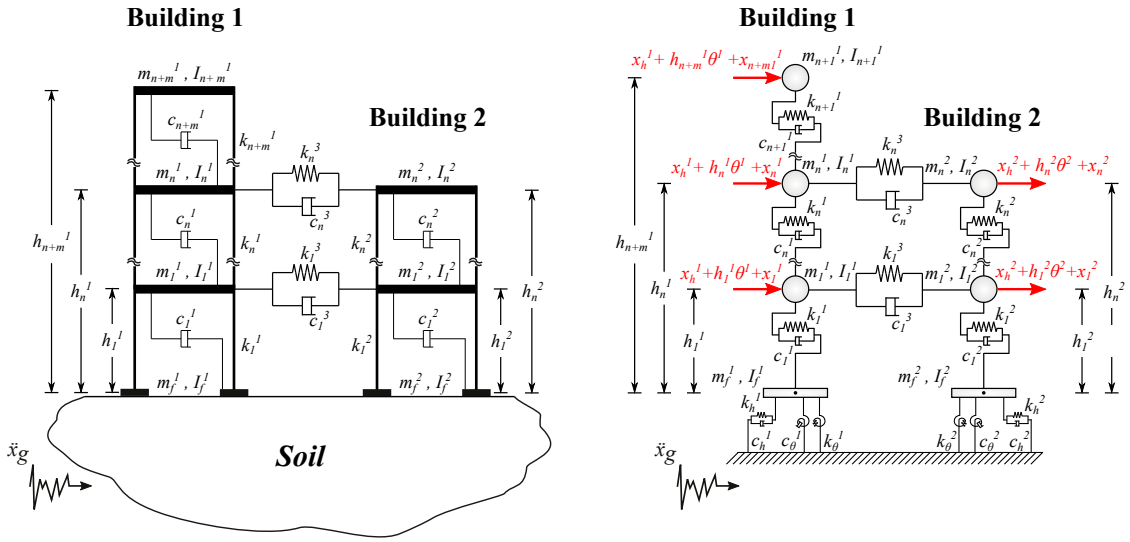

Figure 3. Coupled models of the lumped-mass planar system considering SSI

The equations of motion of the system of Fig. 3 are given by

$$\mathbf{M}_{bsb}\ddot{\mathbf{x}}_{bsb}(t) + \mathbf{C}_{bsb}\dot{\mathbf{x}}_{bsb}(t) + \mathbf{K}_{bsb}\mathbf{x}_{bsb}(t) = -\mathbf{G}_{bsb}\ddot{\mathbf{x}}_g(t) \tag{10}$$

where: the subscript *bsb* in these matrices refers to adjacent buildings considering SSI effects; $\mathbf{M}_{bsb}$, $\mathbf{C}_{bsb}$ and $\mathbf{K}_{bsb}$ are mass, damping and stiffness matrices of the coupled system considering SSI effects, respectively (eq. (11)); $\mathbf{M}^1_{bs}$, $\mathbf{M}^2_{bs}$, $\mathbf{C}^1_{bs}$, $\mathbf{C}^2_{bs}$, $\mathbf{K}^1_{bs}$ and $\mathbf{K}^2_{bs}$ are the mass, damping and stiffness matrices of the *Buildings 1* and *2* considering SSI effects. These matrices must be calculated using eqs. (6) and (7); $\hat{\mathbf{c}}$ and $\hat{\mathbf{k}}$ are the matrices that contains the damping and stiffness coefficients of the linking system c^3_n e k^3_n; $\mathbf{G}$ is the external force location matrix (eq. (12)); $\mathbf{x}_{bsb}(t)$ is the vector with displacements of the structures and foundations eq. (13).

$$\mathbf{M}_{bsb} = \begin{bmatrix} \mathbf{M}^1_{bs} & \mathbf{0} \\ \mathbf{0} & \mathbf{M}^2_{bs} \end{bmatrix} \quad \mathbf{C}_{bsb} = \begin{bmatrix} \mathbf{C}^1_{bs} & -\hat{\mathbf{c}} \\ -\hat{\mathbf{c}} & \mathbf{C}^2_{bs} \end{bmatrix} \quad \mathbf{K}_{bsb} = \begin{bmatrix} \mathbf{K}^1_{bs} & -\hat{\mathbf{k}} \\ -\hat{\mathbf{k}} & \mathbf{K}^2_{bs} \end{bmatrix} \tag{11}$$

$$\mathbf{G}_{bsb} = \mathbf{M}_{bsb} \begin{bmatrix} \mathbf{0} \\ \mathbf{1} \\ \mathbf{0} \\ \mathbf{1} \end{bmatrix} + \begin{bmatrix} \mathbf{v}_s^1 \\ \mathbf{0} \\ \mathbf{v}_s^2 \\ \mathbf{0} \end{bmatrix}, \quad \mathbf{v}_s^j = \begin{bmatrix} 0 \\ m_f^j \end{bmatrix} \; for\; 1 \leq j \leq 2 \tag{12}$$

$$\mathbf{x}_{bsb} = \begin{bmatrix} x_\theta^1(t) & x_h^1(t) & x_1^1(t) & \cdots & x_{n+m}^1(t) & x_\theta^2(t) & x_h^2(t) & x_1^2(t) & \cdots & x_n^2(t) \end{bmatrix}^T \tag{13}$$

2.4 First-order state-space model

From the second-order model (eqs. (1) and (10)), a first-order state-space model can be derived

$$\begin{cases} \dot{\mathbf{z}} = \mathbf{A}\mathbf{z}(t) + \mathbf{E}\ddot{\mathbf{x}}_g(t) \\ \mathbf{y}(t) = \mathbf{C}_y\mathbf{z}(t) \end{cases} \tag{14}$$

$$\mathbf{z}(t) = \begin{bmatrix} \mathbf{x}(t) \\ \dot{\mathbf{x}}(t) \end{bmatrix} \; \mathbf{A} = \begin{bmatrix} \mathbf{0} & \mathbf{I} \\ -\mathbf{M}^{-1}\mathbf{K} & -\mathbf{M}^{-1}\mathbf{C} \end{bmatrix} \; \mathbf{E} = \begin{Bmatrix} \mathbf{0} \\ -\mathbf{1} \end{Bmatrix} \tag{15}$$

In eq. (14), $\dot{\mathbf{z}}$ represents the state of the structural system which contains the relative velocity and responses to acceleration of the two buildings, $\mathbf{z}(t)$ is the state vector, $\mathbf{A}$ corresponds to the matrix system state and $\mathbf{E}$ is the disturbance input matrix (eq. (15)). In addition to the state variables, one different output variable is considered in this work: *inter-story drifts*. The inter-story drifts are the relative displacements between consecutive floors of the same building, and can be defined as

$$\begin{cases} \Delta_1^j = x_1^j(t) \\ \Delta_i^j = x_i^j(t) - x_{i-1}^j(t), \quad 1 < i < n_j \end{cases} \tag{16}$$

where n_j represents the number of stories of the *j*th building (for $1 \leq j \leq 2$). Thus, the vector of inter-story drifts $\mathbf{y}_d(t)$ (eq. (18)) can be obtained using the following output matrix $\mathbf{C}_y$ in eq. (14)

$$\mathbf{C}_y = \begin{bmatrix} \mathbf{Q}_{n+m,n+m}^1 & \mathbf{0} & \mathbf{0} \\ \mathbf{0} & \mathbf{Q}_{n,n}^2 & \mathbf{0} \end{bmatrix} \quad \mathbf{Q}^j = \begin{bmatrix} 1 & & & & \\ -1 & 1 & & & \\ & -1 & 1 & & \\ & & \ddots & \ddots & \\ & & & -1 & 1 \end{bmatrix}, \; for\; 1 \leq j \leq 2 \tag{17}$$

$$\mathbf{y}_d = \begin{bmatrix} \Delta_1^1(t) & \cdots & \Delta_{n+m}^1(t) & \Delta_1^2(t) & \cdots & \Delta_n^2(t) \end{bmatrix}^T \tag{18}$$

3 Numerical Analysis

The structural system studied in this work consists of two shear-frame building (see Fig. 4) whose mechanical properties are taken from [26]. Building 1 is a three-story frame with floor mass $m^1 = 1.20 \times 10^6\ kg$, story stiffness $k^1 = 2.4 \times 10^9\ Nm^{-1}$ and floor height $h^1 = 3.0\ m$. Building 2 is a six-story building with $m^2 = m^1$, story stiffness $k^2 = 2.0 \times 10^9\ Nm^{-1}$ and floor height $h^2 = h^1$. The damping matrices have been computed using the Rayleigh damping method by setting a 2% of relative damping on the corresponding first and last modes.

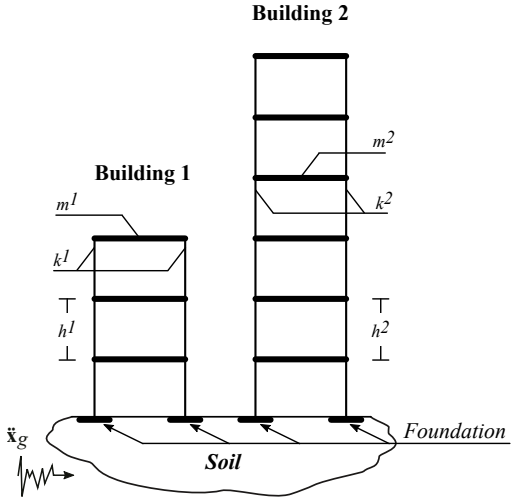

Figure 4. Numerical models of adjacent connected buildings

3.1 First stage

In this stage, adjacent buildings of Fig. 4 are supported on a fixed base and are linked through spring-damper devices. Initially, it was performed an optimization study using Particle Swarm Optimization (PSO) [23]. PSO is a technique used to explore the search space of a given problem to find the settings or parameters required to maximize or minimize a particular objective (fitness function). In this work, PSO is used to minimize the maximum inter-story drift of both buildings in order to calculate the optimal placement of connection device and the k^3 and c^3 optimal values. Stiffness and damping values k^3 and c^3 varied from zero to $30 \times 10^6\ Nm^{-1}$ and $30 \times 10^6\ Nsm^{-1}$, respectively. These values were based on passive dampers properties available commercially. The value $k^3 = 0$ and $c^3 = 0$ indicates that no linking element exists at the nth level between the buildings. Attending to the number and location of the linking devices, seven different configurations of the linking system are possible which are schematically displayed in Fig. 5. Cases (a) – (f) are semi-coupled configurations (not all the floors are connected) and Case (g) is considered a full-coupled system.

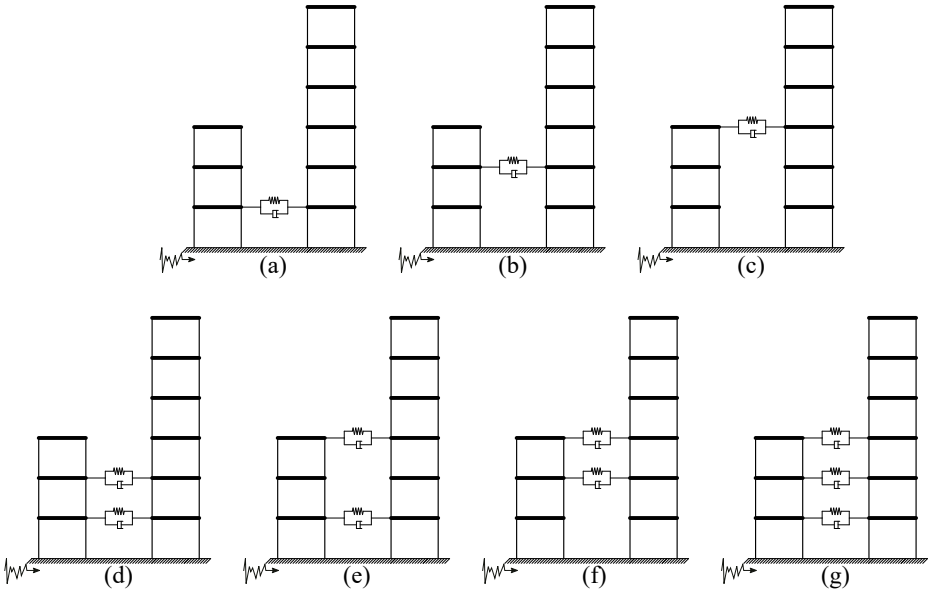

Figure 5. Passive coupling configurations

To solve the system a *fitness* or *objective function* was defined, formed by the sum of the squares of the maximum inter-story drift (Δ) of the two buildings (eq. (19)). Fig. 6 shows the values of the objective functions obtained in the optimization process and for each configuration shown in Fig. 5. Table 1 shows the optimal values for the coefficients k^3 and c^3.

$$f_{objective} = max(\Delta_i^1(t))^2 + max(\Delta_i^2(t))^2 \tag{19}$$

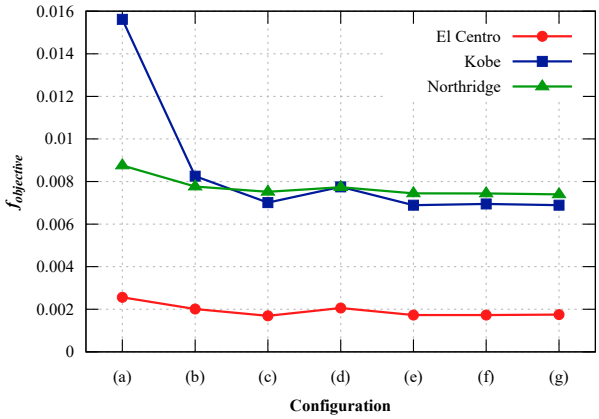

Figure 6. Objective functions values obtained with PSO method – without SSI

Table 1. Optimum values obtained using PSO

Config.	El Centro			Kobe		
	$f_{objective}$	c^3 $[Nsm^{-1}]$	k^3 $[Nm^{-1}]$	$f_{objective}$	c^3 $[Nsm^{-1}]$	k^3 $[Nm^{-1}]$
(a)	0.00256	30×10^6	15.9×10^{-7}	0.01562	30×10^6	37.7×10^{-4}
(b)	0.00201	30×10^6	25.9×10^{-7}	0.00825	30×10^6	47.3×10^{-4}
(c)	0.00169	22.2×10^6	95.9×10^{-7}	0.00701	25.7×10^6	37.7×10^{-4}
(d)	0.00206	21.3×10^6	15.9×10^{-7}	0.00775	30×10^6	37.7×10^{-4}
(e)	0.00173	21.2×10^6	35.5×10^{-7}	0.00689	21.9×10^6	37.7×10^{-4}
(f)	0.00173	13.4×10^6	55.3×10^{-7}	0.00695	17.4×10^6	47.3×10^{-4}
(g)	0.00175	12.0×10^6	85.6×10^{-7}	0.00689	15.4×10^6	47.3×10^{-4}

Config.	Northridge		
	$f_{objective}$	c^3 $[Nsm^{-1}]$	k^3 $[Nm^{-1}]$
(a)	0.00875	30×10^6	33.1×10^{-4}
(b)	0.00777	30×10^6	10.1×10^{-4}
(c)	0.00752	22.7×10^6	33.1×10^{-4}
(d)	0.00773	27.6×10^6	23.8×10^6
(e)	0.00745	25.6×10^6	33.1×10^{-4}
(f)	0.00744	17.5×10^6	30.0×10^6
(g)	0.00740	18.5×10^6	16.9×10^6

It can be observed in Fig. 6 and Table 1 that, for the three earthquakes, Case (a) had high values of the objective function. Likewise, it is possible to notice that the objective function values had a little variation from Case (c) to Case (g). Consequently, it can be said that no significant increase in seismic protection results when more dampers are added. This agrees with other studies [6–11]. Thus, the best configuration is the Case (c) where one single connection device placed at the top level in the minor structure is required. It can be observed in Table 1 that k^3 is approximately zero. Therefore, it can be said that the best connection device to the analyzed model is using only a viscofluid damper.

Next, the natural frequencies and periods for uncoupled and coupled building are calculated by solving the eigenvalues problem $\mathbf{K\Phi} = \lambda\mathbf{M\Phi}$, where $\mathbf{K}$, $\mathbf{M}$, λ and $\mathbf{\Phi}$ represent the mass matrix, stiffness matrix, eigenvalues, and eigenvector values, respectively. Similarly, the inter-story drift for uncoupled and coupled building using optimum values of c^3 and k^3 are calculated. These results are presented in Table 2 and Fig. 7.

An advantage of using viscofluid dampers as a connecting element is that the frequencies and periods of neighboring buildings does not change [6–11]. Thereby, the fundamental frequency of the coupled system will be the lowest value calculated for the two adjacent buildings as seen in Table 2 . Looking at the inter-story drifts in Fig. 7 it is possible to notice that all responses presented a significant reduction (about 40%) due to the connection device installation.

Table 2. Natural frequencies and vibration periods of uncoupled and coupled system without SSI

		$f\ [Hz]$	$T\ [s]$
Uncoupled System	*Building 1*	3.17	0.32
	Building 2	1.57	0.64
Coupled System	–	1.57	0.64

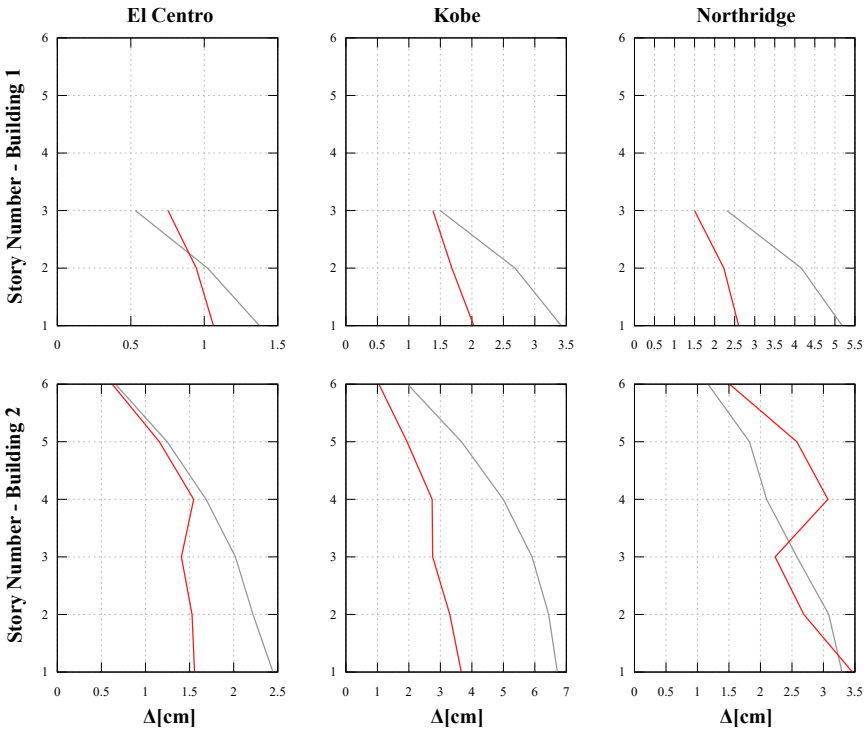

Figure 7. Inter-story drifts of uncoupled and coupled system without SSI

3.2 Second stage

At this stage, the dynamics responses of the coupled model with flexible base are obtained making use of the optimum parameters of the connecting device calculated in the first stage previously. Next, the responses obtained on the first and second stages are compared, to evaluate SSI effects on coupled structures analysis. The coupled model considering SSI is like the one shown on Fig. 3. In this work, the foundation is treated as a circular rigid disk with radius *r* and its flexibility is not considered. According to [15], for typical buildings the practical relationship between the foundation mass and the total mass of the *j*th structure is $0.2 \leq m_f^j/M^j \leq 0.5$. This relationship was used for obtaining the mass of foundation. Likewise, the ratio of the total height of the superstructure to the foundation radius, i.e., h^j/r can be assumed. In this paper, values of $m_f^j/M^j = 0.3$ and h_j/r 1, 2 and 3 are assigned.

Soil types are chosen between soft to hard soils within the range of $160 - 800\ ms^{-1}$ of shear wave velocity of soil V_S. The more resistant the soil is, higher the velocity of propagation of seismic waves V_S is. The mass density of soil ρ which depends on shear-wave velocity is assumed to be 2.35×10^3 and $1.95 \times 10^3 kgm^{-3}$ for shear-wave velocity greater and less than $750\ ms^{-1}$, respectively. Finally, the Poisson's ratio of soil ν considered was 0.4. With this information, it is possible to calculate the soil impedance coefficients (eq. (4)).

Initially, variation of the fundamental period and fundamental frequency of the coupled buildings with dif-

ferent soil shear wave velocity are calculated. The results are shown on Fig. 8. It is observed from this figure that considering the soil makes the modal periods longer. How softer the soil, how longer the period is, consequently, the buildings become more flexible. However, for lower h_j/r ratio, the frequencies and periods of the coupled system are close to those calculated for the same system, but on a fixed basis, being an expected behavior [13–16].

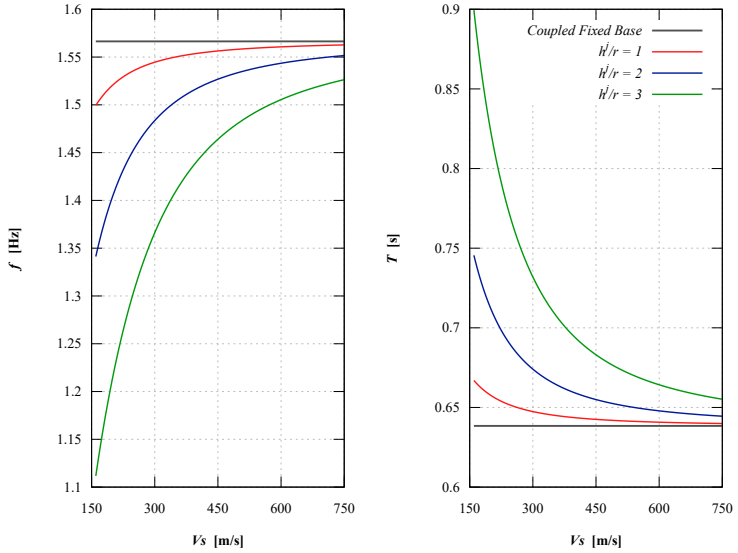

Figure 8. Variation of frequencies and periods of coupled buildings with and without SSI

Next, the *inter-story* drifts of the coupled models on a fixed and flexible basis were compared to visualize the SSI influence on the control performance of the CCM. The responses were normalized in relation to those obtained for the coupled model and supported on a fixed base. The results are illustrated in Fig. 9.

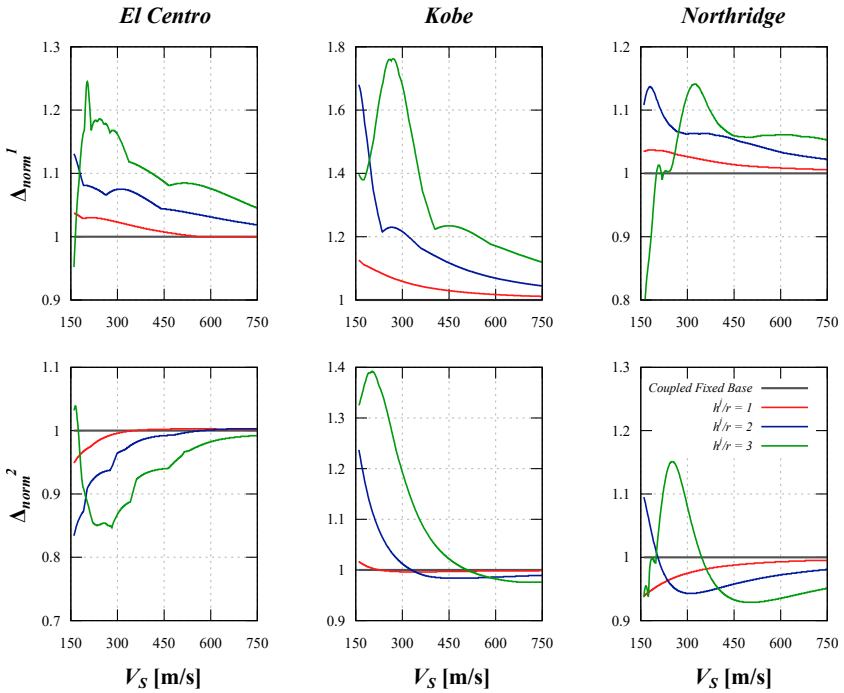

Figure 9. Variation of normalized *inter-story* drifts of coupled structures with and without SSI

It can be seen in Fig. 9 that the consideration of the soil in the analysis increased the maximum *inter-story* drift in the coupled buildings, and for the Kobe earthquake these increments were greater than 60% in Building 1 and 40% in Building 2. Similarly, it is possible to observe that the higher the h_j/r ratio, the longer is *inter-story* drift. There are two likely explanations. First, the consideration of the soil in the analysis added the values of the fundamental period of the coupled model, which makes the buildings more flexible. Second, this increment is

because of additional displacements imposed to the building by the horizontal component of the soil [5]. First story displacement is increased due to this component which causes larger relative displacements between foundation level and this story and consequently larger inter-story drift.

In Fig. 9 it is also possible to observe the importance of the superficial foundation size ($h_j/r < 2$), because the greater the size of the shallow foundation, the closer the results of the coupled models without and with SSI become, and the soil can be disregarded from the analysis, and the connection properties values calculated in the first step are efficient.

4 Conclusions

The influence of soil-structure interaction on the behavior of two neighboring buildings interconnected by means of viscofluid dampers was presented. An example case of structures with known and fixed mechanical properties was used. The interaction between soil and structure was represented by a discrete model of springs and dampers. The buildings were considered to be supported on circular superficial foundation.

It was found that when considering the SSI effects, there is a modification in the values of the frequency and the fundamental period of the coupled system that resulted in greater displacements during the seismic excitation. The more rigid the soil, the responses of the coupled model considering the SSI is similar to the results of the fixed base model, being an expected behavior. In the same way, it can be said that the larger the superficial foundation size or the smaller the h_j/r ratio, the greater the possibility of disregarding the SSI effect in the numerical analysis.

Likewise, it was demonstrated that a new optimization study should be carried out when considering SSI and it is not possible to use the optimization results considering the model supported on a fixed basis for $V_S < 450\, ms^{-1}$. However, if a new optimization study is not possible, it can be said that a possible solution would be to use a viscoelastic damper $\left(k^3 \neq 0\right)$ as a connection element. This type of device can change the fundamental period and frequency of the coupled system and thus be able to decrease its dynamic responses [2–11]. Since the consideration of SSI in the model makes these responses depend on the frequency components associated with seismic excitation. Another solution would be to implement active or semi-active control systems lonely in each of these buildings that assist in controlling these responses. Additional studies on setting connecting device properties are necessary, considering on optimization procedures the SSI effects.

Acknowledgements. The authors acknowledge CNPq Brazilian Council of National Scientific and Technological Development and Federal District Research Support Foundation (FAPDF) for the financial support of this research.

Authorship statement. The authors hereby confirm that they are the sole liable persons responsible for the authorship of this work, and that all material that has been herein included as part of the present paper is either the property (and authorship) of the authors, or has the permission of the owners to be included here.

References

[1] R. Klein, C. Cusano, and J. Stukel. Investigation of a method to stabilize wind induced oscillations in large structures. *ASME Winter Annual Meeting*, vol. , 1972.

[2] B. Westermo. The dynamics of interstructural connection to prevent pounding. *Earthquake engineering & structural dynamics*, vol. 18, n. 5, pp. 687–699, 1989.

[3] M. Barbato and E. Tubaldi. A probabilistic performance-based approach for mitigating the seismic pounding risk between adjacent buildings. *Earthquake Engineering & Structural Dynamics*, vol. 42, n. 8, pp. 1203–1219, 2013.

[4] E. Tubaldi, M. Barbato, and S. Ghazizadeh. A probabilistic performance-based risk assessment approach for seismic pounding with efficient application to linear systems. *Structural Safety*, vol. 36, pp. 14–22, 2012.

[5] S. Naserkhaki and H. Pourmohammad. Ssi and sssi effects in seismic analysis of twin buildings: discrete model concept. *Journal of Civil Engineering and Management*, vol. 18, n. 6, pp. 890–898, 2012.

[6] E. Tubaldi. Dynamic behavior of adjacent buildings connected by linear viscous/viscoelastic dampers. *Structural Control and Health Monitoring*, vol. 22, n. 8, pp. 1086–1102, 2015.

[7] L. Perez, S. Avila, and G. Doz. *Seismic response control of adjacent buildings connected by viscous and hybrid dampers*. Springer, 2014.

[8] C. Patel and R. Jangid. Dynamic response of identical adjacent structures connected by viscous damper. *Structural Control and Health Monitoring*, vol. 21, n. 2, pp. 205–224, 2014.

[9] F. Palacios-Quiñonero, J. Rossell, J. Rubio-Massegú, and H. Karimi. Structural vibration control for a class of connected multistructure mechanical systems. *Mathematical Problems in Engineering*, vol. 2012, 2012a.
[10] H. Roh, G. Cimellaro, and D. Lopez-Garcia. Seismic response of adjacent steel structures connected by passive device. *Advances in Structural Engineering*, vol. 14, n. 3, pp. 499–517, 2011.
[11] H. Zhu, D. Ge, and X. Huang. Optimum connecting dampers to reduce the seismic responses of parallel structures. *Journal of Sound and Vibration*, vol. 330, n. 9, pp. 1931–1949, 2011.
[12] J. Wolf. *Dynamic soil-structure interaction*. Prentice Hall, 1987.
[13] W. Xiong, L. Jiang, and Y. Li. Influence of soil–structure interaction (structure-to-soil relative stiffness and mass ratio) on the fundamental period of buildings: experimental observation and analytical verification. *Bulletin of Earthquake Engineering*, vol. 14, n. 1, pp. 139–160, 2016.
[14] B. Jayalekshmi and H. Chinmayi. Soil–structure interaction effect on seismic force evaluation of rc framed buildings with various shapes of shear wall: as per is 1893 and ibc. *Indian Geotechnical Journal*, vol. 45, n. 3, pp. 254–266, 2015.
[15] E. A. F. Khoshnoudian and M. Hosseini. Importance of soil material damping in seismic responses of soil-mdof structure systems. *Soils and Foundations*, vol. 55, n. 1, pp. 35–44, 2015.
[16] G. Hatzigeorgiou and G. Kanapitsas. Evaluation of fundamental period of low-rise and mid-rise reinforced concrete buildings. *Earthquake engineering & structural dynamics*, vol. 42, n. 11, pp. 1599–1616, 2013.
[17] A. Farghaly. Optimization of viscous dampers with the influence of soil structure interaction on response of two adjacent 3-d buildings under seismic load. *Optimization*, vol. 4, n. 1, 2014.
[18] N. Alexander, E. Ibraim, and H. Aldaikh. A simple discrete model for interaction of adjacent buildings during earthquakes. *Computers & Structures*, vol. 124, pp. 1–10, 2013.
[19] H. Aldaikh, N. Alexander, E. Ibraim, and O. Oddbjornsson. Two dimensional numerical and experimental models for the study of structure–soil–structure interaction involving three buildings. *Computers & Structures*, vol. 150, pp. 79–91, 2015.
[20] E. Kausel. Early history of soil–structure interaction. *Soil Dynamics and Earthquake Engineering*, vol. 30, n. 9, pp. 822–832, 2010.
[21] G. Gazetas. Formulas and charts for impedances of surface and embedded foundations. *Journal of geotechnical engineering*, vol. 117, n. 9, pp. 1363–1381, 1991.
[22] S. Tileylioglu, J. Stewart, and R. Nigbor. Dynamic stiffness and damping of a shallow foundation from forced vibration of a field test structure. *Journal of Geotechnical and Geoenvironmental Engineering*, vol. 137, n. 4, pp. 344–353, 2011.
[23] J. Kennedy and R. Eberhart. Particle swarm optimization. In *Proceedings of ICNN'95-international conference on neural networks*, volume 4, pp. 1942–1948. IEEE, 1995.
[24] J. Bowles. *Foundation Analysis and design*. McGraw Hills, 1998.
[25] J. Wolf. *Foundation vibration analysis: A strength of materials approach*. Elsevier, 2004.
[26] F. Palacios-Quiñonero, J. Rossell, J. Rubio-Massegú, and H. Karimi. Semiactive-passive structural vibration control strategy for adjacent structures under seismic excitation. *Journal of the Franklin Institute*, vol. 349, n. 10, pp. 3003–3026, 2012b.